WPMAT-CPR(17) 16947

Y Mao et al.

Development and characterization of powder metallurgically produced random discontinuous tungsten fiber reinforced tungsten composites

Preprint of Paper to be submitted for publication in Proceeding of 16th International Conference on Plasma-Facing Materials and Components for Fusion Applications

This work has been carried out within the framework of the EUROfusion Consortium and has received funding from the Euratom research and training programme 2014-2018 under grant agreement No 633053. The views and opinions expressed herein do not necessarily reflect those of the European Commission.

Development and characterization of powder metallurgically produced discontinuous tungsten fiber reinforced tungsten composites

Y.Mao[a], J.W.Coenen[a], J.Riesch[b], S.Sistla[c], J.Almanstötter[d], B.Jasper[a], A.Terra[a], T.Höschen[b], H.Gietl[b,e], M. Bram[f], J. Gonzalez-Julian[f], Ch.Linsmeier[a] and Ch.Broeckmann[c]

[a] Institut für Energie und Klimaforschung – Plasmaphysik, Forschungszentrum Jülich GmbH, 52425 Jülich, Germany

[b] Max-Planck-Institut für Plasmaphysik, 85748 Garching b. München, Germany

[c] Institut für Werkstoffanwendungen im Maschinenbau (IWM), RWTH Aachen University, 52062 Aachen, Germany

[d]OSRAM GmbH, SP PRE PLM DMET, Mittelstetter Weg 2, 86830 Schwabmünchen, Germany

[e]Technische Universität München, Boltzmannstrasse 15, 85748 Garching, Germany

[f] Institut für Energie und Klimaforschung - Materials Synthesis and Processing, Forschungszentrum Jülich GmbH, 52425 Jülich, Germany

Abstract: In future fusion reactors, tungsten is the prime candidate material for the first wall and the divertor. Nevertheless, the intrinsic brittleness of tungsten is a major concern with respect to the fusion environment with thermal fatigue by high transient heat loads and strong particle bombardment. Intense neutron radiation can lead to further embrittlement e.g. transmutation or irradiation hardening and are, therefore, crucial to material performance.

To overcome this drawback, tungsten fiber reinforced tungsten (W_f/W) composites are being developed relying on an extrinsic toughing principle. Similar to those in ceramic matrix composite, with the help of the extrinsic mechanism, e.g. fracture deflection and fiber pull-out, as energy dissipation mechanism, the W_f/W composites represent a pseudo ductile behavior and damage resilient capability. The optimization of the chosen interface (Y_2O_3) between the fiber and matrix, is crucial to active the pseudo ductility mechanisms.

Recent developments in the area of discontinuous powder-metallurgical W_f/W will be presented showing a possible path towards a component based on standard tungsten production technologies, such as field assisted sintering technology (FAST) and hot isostatic pressing (HIP). Initial mechanical tests and microstructural analyses show potential for pseudo-ductile behavior at room temperature of FAST and HIP produced W_f/W materials with a fiber volume fraction of 30%.

1. Introduction

Tungsten is currently the main candidate material for plasma facing component in future fusion reactors due to its resistance against erosion, high melting point, benign activation behavior by neutron irradiation, and low tritium retention [1, 2]. However, the main concern when using tungsten is its intrinsic brittleness. Under the extreme conditions of fusion environment with high transient heat loads and neutron irradiation, a tungsten plasma facing material will face the possibility of crack formation during operation and subsequent catastrophic failure [3]. Tungsten fiber reinforced tungsten (W_f/W) composites have been developed to overcome this issue, relying on extrinsic toughing mechanisms by using commercially available tungsten wires as reinforcement [4-6]. By incorporation of the fibers, fiber pull-out, ductile deformation of the fibers, crack deflection and interface de-bonding can act as energy dissipation mechanism during crack propagation. These mechanisms enable W_f/W to behave pseudo ductile [7], similar to ceramic matrix composites [8-10]. The crucial factor to realize pseudo ductility is the existence of a relatively weak fiber-matrix interface [11-13].

The two potential methods to manufacture W_f/W composites are chemical vapor deposition (CVD) [7, 14] and powder metallurgy processes (PM) [15-18]. Both production routes have shown

the possibility to achieve the expected pseudo ductility. Compared to the CVD production route, the PM process, as a more mature industrial process, has several benefits, such as substantial experience with bulk production, higher sample density and an easier realization of alloy production. However, the potential issue for the PM process is that, the high temperature during sintering will cause recrystallization of the as drawn microstructure in tungsten fiber and, hence, weaken the fibers ductility and strength [5, 19]. Additionally, the fiber-matrix interface will be damaged due to the high temperature and pressure during the consolidation process [15, 20].

In this work, discontinuous W_f/W samples were prepared via different PM processes: Field assisted sintering technology (FAST) [21-25] and hot isostatic pressing (HIP) [26-28]. The study focuses on the microstructure and load capability of the PM produced W_f/W.

2. W_f/W manufacturing and microstructure

The raw materials of the W_f/W composites fabrication are pure tungsten powders (provided by OSRAM GmbH) with 5 µm average particle size (fischer sub sieve size) and potassium doped short tungsten fibers (provided by OSRAM GmbH) with 2.4mm length and 0.24mm diameter. The tungsten fibers were produced by a drawing process and then cut into the required length. Due to the drawn microstructure with elongated grains, the tungsten fibers show ductile behavior and extremely high tensile strength (~3000 MPa) [5, 19]. Since potassium is insoluble in tungsten the doping (approx. 75 ppm) is present in form of nano-disperse rows of bubbles along the elongated grains pinning the grain boundaries and thus leading to a good high temperature microstructure stability [5].

Before the FAST and HIP process, the tungsten fibers were coated with a 2.5 µm yttria layer to form a dedicated fiber-matrix interface, by using a magnetron sputtering process (Fig. 1). Coating

production details are shown in [20]. In a next step, the tungsten fibers were mixed with the tungsten powders by manual shaking in a vessel with a fiber volume fraction of 30%. The similar density of the tungsten powders and the tungsten fibers leads to a random distribution of the tungsten fibers in the mixture.

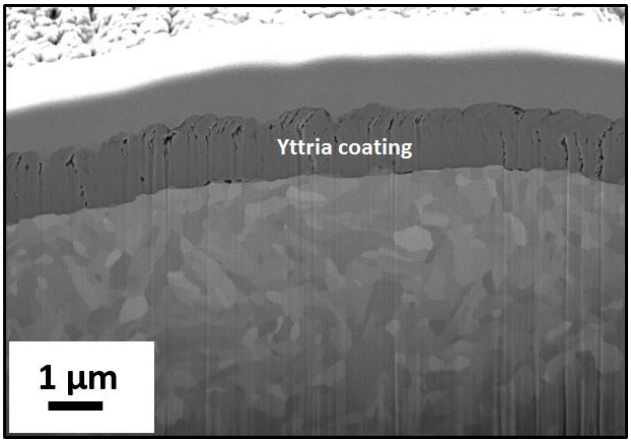

Fig: 1 SEM image of thin film cross section prepared by focused ion beam (FIB) cut showing an yttria thin film structure (the visible additional top layer of platinum was deposited during sample preparation for FIB cut).

The FAST and HIP process parameters are shown in Table 1. Schematic diagrams of the processes are shown in Fig. 2. During the FAST process, the powder/fiber mixture was consolidated in a graphite die with 20 mm inner diameter. The sintering was performed under vacuum below 0.1 mbar. As result, coin shape samples (20 mm diameter and ~5 mm height) was produced (Fig. 3). For the HIP process, the powder/fiber mixture was firstly uniaxial (in z direction in Fig .2) pre-pressed at 200 MPa and then put into a tantalum capsule. After vacuum seal welding, the tantalum capsule was then consolidated in the HIP chamber. The isostatic pressure was applied by means of an Argon gas inlet. The HIP sample after consolidation is cylindrical in shape with ~18 mm diameter and ~14 mm height (Fig. 3).

The mass density of the sintered W_f/W samples after consolidation was measured by the Archimedes principle. The results are given in Table. 1.

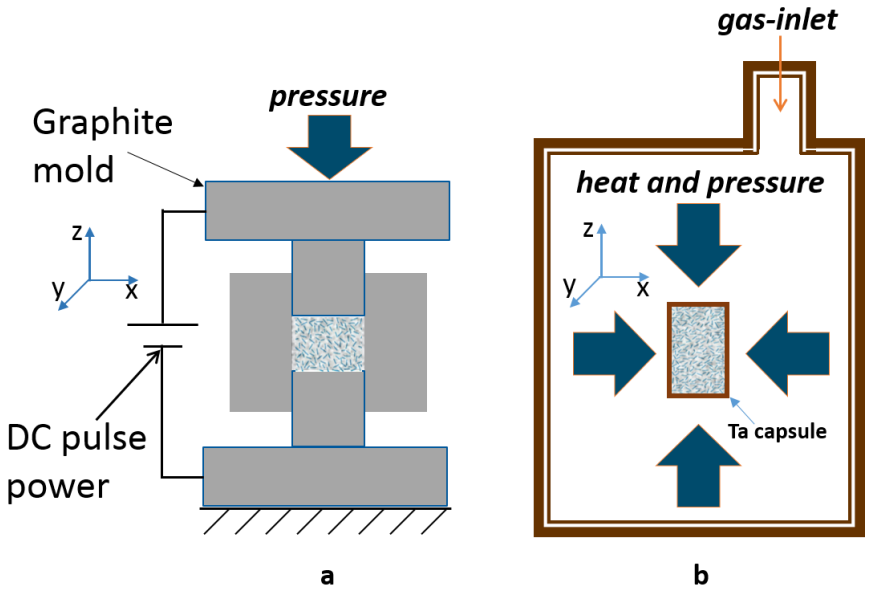

Fig. 2: Schematic diagram of FAST (a) and HIP (b) processes.

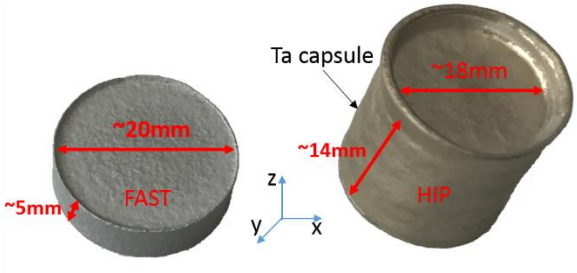

Fig. 3: Representative W_f/W samples after powder metallurgical consolidation.

Table. 1: FAST and HIP process parameters and relative density of the samples.

	Temperature	Pressure	Holding time	Heating rate	Relative density
FAST	1900 °C	60 MPa	4 min	200 K/min	~94%
HIP	1600 °C	200 MPa	2 h	10 K/min	~98%

Fig. 4 and 5 represent the overview microstructure of the as-fabricated W_f/W. The cross sections shown are parallel and perpendicular to z axis, respectively. A relatively homogeneous fiber

distribution can be observed in all cases. Potential fiber distribution inhomogeneity could be caused by insufficient shaking during mixing or punch/capsule compression during sintering.

The samples from both processes tend to have a 2-dimentional planar fiber orientation distribution. Most fibers tend to orient parallel to x-y plane. For the FAST process, it is assumed to be due to the height reduction in the z-direction during sintering. For the HIP process, it is caused by the uniaxial pre-pressing (in z direction) during green body preparation. Additionally, fiber deformation after consolidation is visible, especially when fibers are in contact with each other, as marked in Fig. 5.

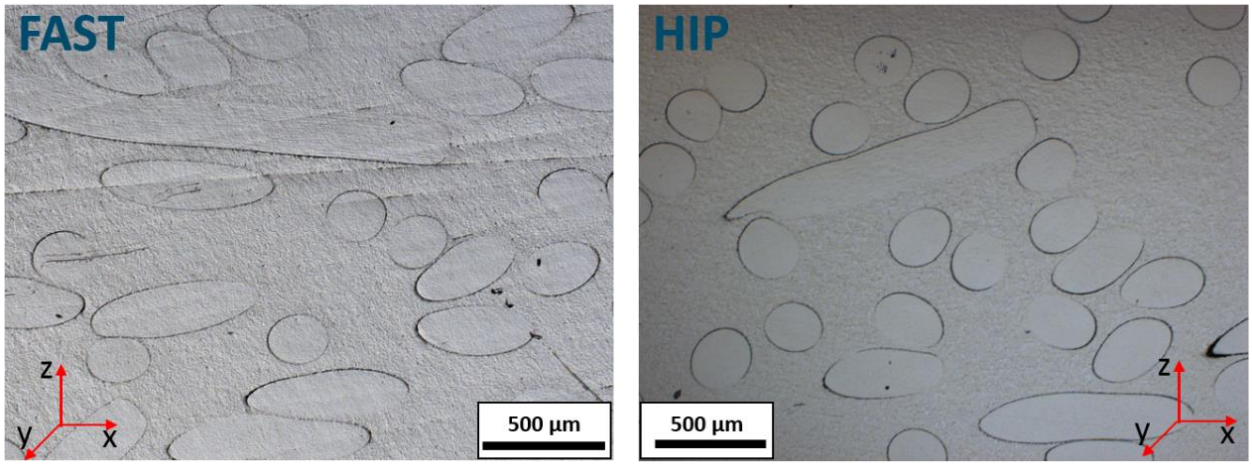

Fig. 4: Light microscope image of the overview microstructure of the FAST and HIP produced W_f/W, the cross sections are parallel to z axis.

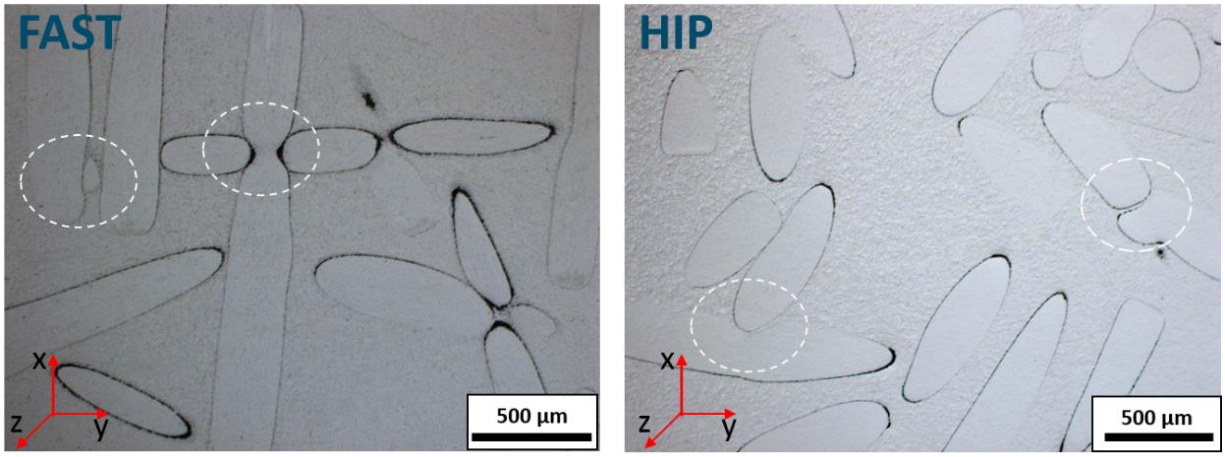

Fig. 5 Light microscope image of the overview microstructure of the FAST and HIP produced W_f/W, the cross sections are perpendicular to z axis.

Fig. 6 represents the detailed view of the fiber-matrix interface region. The fiber-matrix interfaces are visible after sintering for the samples from both processes. However, in contrast to the dense and homogenous occurrence of the yttria layer in the as-coated state in Fig. 1, the yttria interface got damaged during the consolidation process. Especially the outer shell of the interface got penetrated by the tungsten powders owing to the external pressure and the high temperature [15, 20, 29, 30]. The interface damage during the FAST product looks more severe (Fig. 6), probably due to the higher process temperature. Also the reported dielectric breakdown effect for the electrically isolating yttria interface might play a role [29, 30].

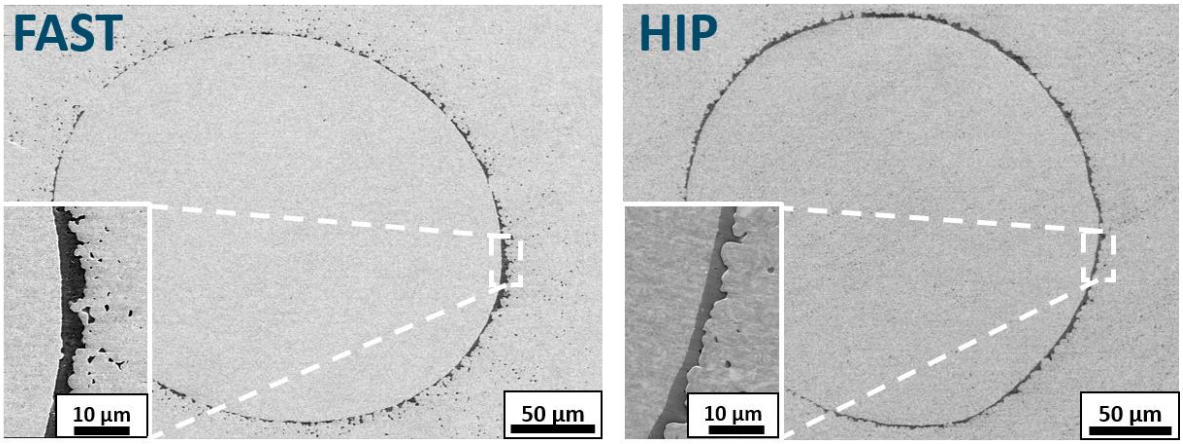

Fig. 6: SEM images of the Fiber-matrix interface region of the FAST and HIP produced W_f/W composites.

3. Fracture behavior

To observe the crack propagation behavior of the W_f/W composites, a pre-notched 3-point bending test was performed at room temperature (RT) on samples produced by the above described processes. Sample dimensions were 18 x 2 x 4 mm^3 (length x width x thickness) with a ~2 mm deep notch. The pre-notch was prepared by diamond wire cutting followed by manually razor blade polishing. The bending tests were performed with an Instron 3342 universal testing machine (Instron GmbH, Darmstadt, Germany) with a displacement rate of 5 µm/s.

Typical load-displacement curves of FAST produced pure W, W_f/W composites and HIP produced W_f/W composites are represented in Fig. 7. It is important to note that, the absolute values of the force in these curves are not directly comparable. Because the pre-notch was manually prepared, therefore, the sharpness and the depth of the notches are not identical. The fracture surfaces of the samples after the pre-notched 3-point bending tests are shown in Fig. 8.

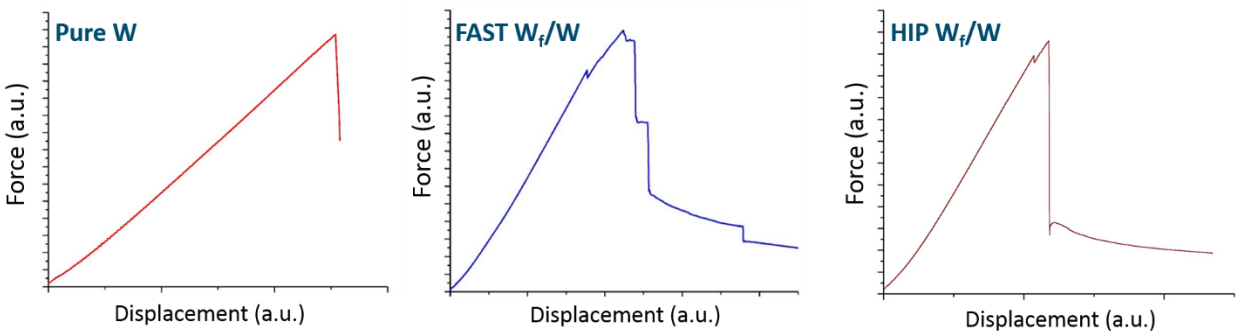

Fig. 7: Typical load-displacement curves of FAST produced pure W, W_f/W and HIP produced W_f/W during pre-notched 3-point bending tests.

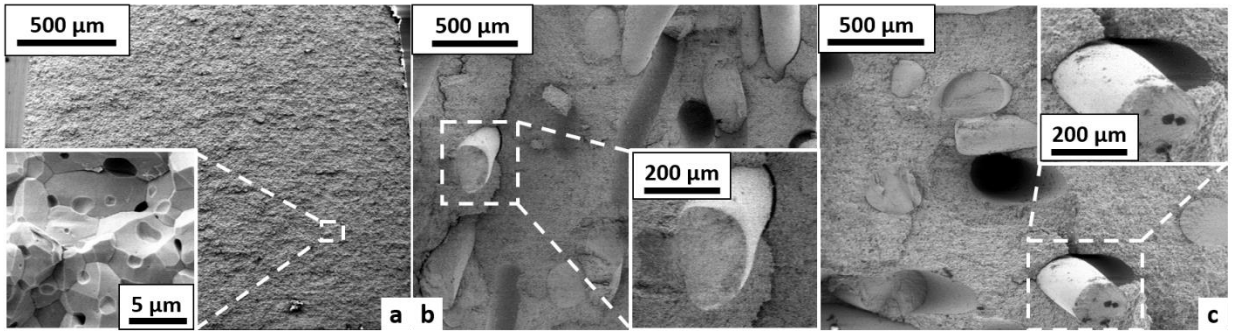

Fig. 8: SEM image of the fracture sections after the pre-notched 3-point bending tests of FAST produced pure W (a), W_f/W (b) and HIP produced W_f/W (c).

As shown in Fig, 7a, at RT, the pure tungsten sample show pure linearly elastic loading until a severe load drop to zero during failure without having any plastic deformation. Also a clear intergranular fracture surface is observed as shown in Fig. 8a.

Both W_f/W samples represent different force-displacement curves compared to pure tungsten: after the first load-drop, the load still increases; a massive load-drop occurs after reaching the maximum load; afterwards, the samples tend to have a stepwise or continuous load-drop instead of a completely failure.

The matrix fracture of the W_f/W composites (not shown here) is also intergranular fracture, same as pure tungsten case. Interface de-bonding, fiber pull-out can be observed in both W_f/W

composites fracture surface, as shown in Fig. 8b and c. Additionally, the overall fracture surface of the W_f/W is more uneven compared to the pure tungsten.

The above results give a strong indication that the PM produced W_f/W composites are able to exhibit typical pseudo ductile behavior similar to CVD produced W_f/W [4]: the first load-drop signifies the matrix failure; after the matrix failure, the load still increases due to the crack bridging by the fibers; the massive load-drop indicates the multiple fiber failure; then the further load bearing capability is supplied by frictional fiber pull-out from the matrix. The uneven fracture surface gives a hint for observed crack deflection. Here the fiber pull-out, fiber elastic bridging and crack deflection are likely the energy dissipation mechanisms which strongly contribute to the elevated load capability compared to pure tungsten [9, 31]. This conclusion will be further detailed in the future study including standard fracture toughness measurements.

4. Conclusion and outlook

~94% and ~98% dense W_f/W composites are able to be produced by FAST and HIP process, respectively. Both processes give similar microstructures after consolidation with homogeneous distributed, 2D-oriented fibers. Fiber-matrix interface remains intact after PM processes. Compared to the pure tungsten, the PM produced W_f/W samples are able to show a pseudo-ductility behavior at RT. The improved load capability relies on the energy dissipation mechanisms like fiber pull-out, crack bridging by the fibers and crack deflection. For the first time pseudo-ductile behavior of a HIP produced W_f/W composite at RT was presented.

The fiber volume fraction influence on the composite properties has also been studied and will be reported in the future. In the next step, the influence of the fiber-matrix interface strength on

the composite will be studied. The W_f/W composites with different interface materials will be produced and analyzed.

Acknowledgement: This work has been carried out within the framework of the EUROfusion Consortium and has received funding from the Euratom research and training program 2014-2018 under grant agreement No 633053. The views and opinions expressed herein do not necessarily reflect those of the European Commission. We would like to also thank Anna Weddeling from Lehrstuhl für Werkstofftechnik Ruhr-Universität Bochum for the assistance with the HIP process.

Reference

[1] V. Philipps, Tungsten as material for plasma-facing components in fusion devices, J. Nucl. Mater., 415 (2011) S2-S9.
[2] J.W. Coenen, S. Antusch, M. Aumann, W. Biel, J. Du, J. Engels, S. Heuer, A. Houben, T. Hoeschen, B. Jasper, F. Koch, J. Linke, A. Litnovsky, Y. Mao, R. Neu, G. Pintsuk, J. Riesch, M. Rasinski, J. Reiser, M. Rieth, A. Terra, B. Unterberg, W. Th, T. Wegener, J.H. You, L. Ch, Materials for DEMO and reactor applications—boundary conditions and new concepts, Physica Scripta, 2016 (2016) 014002.
[3] G. Pintsuk, I. Bobin-Vastra, S. Constans, P. Gavila, M. Rödig, B. Riccardi, Qualification and post-mortem characterization of tungsten mock-ups exposed to cyclic high heat flux loading, Fusion Engineering and Design, 88 (2013) 1858-1861.
[4] J. Riesch, T. Höschen, C. Linsmeier, S. Wurster, J.H. You, Enhanced toughness and stable crack propagation in a novel tungsten fibre-reinforced tungsten composite produced by chemical vapour infiltration, Physica Scripta, T159 (2014) 014031.
[5] J. Riesch, Y. Han, J. Almanstötter, J.W. Coenen, T. Höschen, B. Jasper, P. Zhao, C. Linsmeier, R. Neu, Development of tungsten fibre-reinforced tungsten composites towards their use in DEMO - Potassium doped tungsten wire, in: Physica Scripta, 2016.
[6] R. Neu, J. Riesch, J.W. Coenen, J. Brinkmann, A. Calvo, S. Elgeti, C. García-Rosales, H. Greuner, T. Hoeschen, G. Holzner, F. Klein, F. Koch, C. Linsmeier, A. Litnovsky, T. Wegener, S. Wurster, J.H. You, Advanced tungsten materials for plasma-facing components of DEMO and fusion power plants, Fusion Engineering and Design, 109-111 (2016) 1046-1052.
[7] H. Gietl, J. Riesch, J.W. Coenen, T. Höschen, C. Linsmeier, R. Neu, Tensile deformation behavior of tungsten fibre-reinforced tungsten composite specimens in as-fabricated state, Fusion Engineering and Design, (2017).
[8] K.K. Chawla, Ceramic matrix composites, in: Composite Materials, Springer, 1998, pp. 212-251.

[9] H. Stang, S.P. Shah, Failure of fibre-reinforced composites by pull-out fracture, Journal of Materials Science, 21 (1986) 953-957.
[10] V.C. Li, Y. Wang, S. Backer, A micromechanical model of tension-softening and bridging toughening of short random fiber reinforced brittle matrix composites, J. Mech. Phys. Solids, 39 (1991) 607-625.
[11] J. Du, T. Höschen, M. Rasinski, J.H. You, Shear debonding behavior of a carbon-coated interface in a tungsten fiber-reinforced tungsten matrix composite, J. Nucl. Mater., 417 (2011) 472-476.
[12] J. Du, T. Höschen, M. Rasinski, S. Wurster, W. Grosinger, J.H. You, Feasibility study of a tungsten wire-reinforced tungsten matrix composite with ZrOx interfacial coatings, Composites Science and Technology, 70 (2010) 1482-1489.
[13] J. Du, T. Höschen, M. Rasinski, J.H. You, Interfacial fracture behavior of tungsten wire/tungsten matrix composites with copper-coated interfaces, Materials Science and Engineering: A, 527 (2010) 1623-1629.
[14] J. Riesch, M. Aumann, J.W. Coenen, H. Gietl, G. Holzner, T. Höschen, P. Huber, M. Li, C. Linsmeier, R. Neu, Chemically deposited tungsten fibre-reinforced tungsten – The way to a mock-up for divertor applications, Nuclear Materials and Energy, 9 (2016) 75-83.
[15] J.W. Coenen, Y. Mao, J. Almanstötter, A. Calvo, S. Sistla, H. Gietl, B. Jasper, J. Riesch, M. Rieth, G. Pintsuk, F. Klein, A. Litnovsky, A.V. Mueller, T. Wegener, J.H. You, C. Broeckmann, C. Garcia-Rosales, R. Neu, C. Linsmeier, Advanced materials for a damage resilient divertor concept for DEMO: Powder-metallurgical tungsten-fibre reinforced tungsten, Fusion Engineering and Design, in press.
[16] B. Jasper, J.W. Coenen, J. Riesch, T. Höschen, M. Bram, C. Linsmeier, Powder Metallurgical Tungsten Fiber-Reinforced Tungsten, Materials Science Forum, 825-826 (2015) 125-133.
[17] B. Jasper, S. Schoenen, J. Du, T. Hoeschen, F. Koch, C. Linsmeier, R. Neu, J. Riesch, A. Terra, J.W. Coenen, Behavior of tungsten fiber-reinforced tungsten based on single fiber push-out study, Nuclear Materials and Energy, (2016).
[18] L.H. Zhang, Y. Jiang, Q.F. Fang, T. Zhang, X.P. Wang, C.S. Liu, Toughness and microstructure of tungsten fibre net-reinforced tungsten composite produced by spark plasma sintering, Materials Science and Engineering: A, 659 (2016) 29-36.
[19] J. Riesch, J. Almanstötter, J.W. Coenen, M. Fuhr, H. Gietl, Y. Han, T. Höschen, C. Linsmeier, N. Travitzky, P. Zhao, R. Neu, Properties of drawn W wire used as high performance fibre in tungsten fibre-reinforced tungsten composite, IOP Conference Series: Materials Science and Engineering, 139 (2016) 012043.
[20] Y. Mao, J. Engels, A. Houben, M. Rasinski, J. Steffens, A. Terra, C. Linsmeier, J.W. Coenen, The influence of annealing on yttrium oxide thin film deposited by reactive magnetron sputtering: Process and microstructure, Nuclear Materials and Energy, in press (2017).
[21] D.M. Hulbert, A. Anders, D.V. Dudina, J. Andersson, D. Jiang, C. Unuvar, U. Anselmi-Tamburini, E.J. Lavernia, A.K. Mukherjee, The absence of plasma in “spark plasma sintering”, J. Appl. Phys., 104 (2008) 033305.
[22] O. Guillon, J. Gonzalez-Julian, B. Dargatz, T. Kessel, G. Schierning, J. Räthel, M. Herrmann, Field-Assisted Sintering Technology/Spark Plasma Sintering: Mechanisms, Materials, and Technology Developments, Advanced Engineering Materials, 16 (2014) 830-849.

[23] Y. Kim, K.H. Lee, E.-P. Kim, D.-I. Cheong, S.H. Hong, Fabrication of high temperature oxides dispersion strengthened tungsten composites by spark plasma sintering process, International Journal of Refractory Metals and Hard Materials, 27 (2009) 842-846.
[24] K.N. Allahar, D.P. Butt, J. Webb, I. Charit, Electrochemical properties of spark plasma sintered tungsten, in: NACE - International Corrosion Conference Series, 2011.
[25] R. Ohser-Wiedemann, U. Martin, A. Müller, Fast sintering of mechanical alloyed Mo-W powders, in: Proceedings of the International Euro Powder Metallurgy Congress and Exhibition, Euro PM 2012, 2012.
[26] A.S. Helle, K.E. Easterling, M.F. Ashby, Hot-isostatic pressing diagrams: New developments, Acta Metall., 33 (1985) 2163-2174.
[27] A. Svoboda, H.A. Häggblad, L. Karlsson, Simulation of hot isostatic pressing of a powder metal component with an internal core, Computer Methods in Applied Mechanics and Engineering, 148 (1997) 299-314.
[28] E. Arzt, M.F. Ashby, K.E. Easterling, Practical applications of hotisostatic Pressing diagrams: Four case studies, Metallurgical Transactions A, 14 (1983) 211-221.
[29] C.S. Bonifacio, T.B. Holland, K. Van Benthem, Time-dependent dielectric breakdown of surface oxides during electric-field-assisted sintering, Acta Materialia, 63 (2014) 140-149.
[30] C.S. Bonifacio, T.B. Holland, K. van Benthem, Evidence of surface cleaning during electric field assisted sintering, Scripta Materialia, 69 (2013) 769-772.
[31] J. Riesch, J.Y. Buffiere, T. Höschen, M. di Michiel, M. Scheel, C. Linsmeier, J.H. You, In situ synchrotron tomography estimation of toughening effect by semi-ductile fibre reinforcement in a tungsten-fibre-reinforced tungsten composite system, Acta Materialia, 61 (2013) 7060-7071.